

# Modeling and Analysis of a Flywheel Energy Storage System with a Power Converter Interface

Satish Samineni<sup>1</sup>, Brian K Johnson<sup>2</sup>, Herbert L Hess<sup>3</sup> and Joseph D Law<sup>4</sup>

(1) Dept. of Electrical and Computer Engineering, University of Idaho, Moscow, Idaho, 83844, U.S.A (e-mail: ssatish@ieee.org), (2) Dept. of Electrical and Computer Engineering, University of Idaho, Moscow, Idaho, 83844, U.S.A (e-mail: b.k.johnson@ieee.org), (3) Dept. of Electrical and Computer Engineering, University of Idaho, Moscow, Idaho, 83844, U.S.A (e-mail: hhess@uidaho.edu), (4) Dept. of Electrical and Computer Engineering, University of Idaho, Moscow, Idaho, 83844, U.S.A (e-mail: jlaw@uidaho.edu)

**Abstract** – A shipboard power system is a stiff, isolated power system. Power is generated locally, and distributed over short distances making the system vulnerable to transients. Power quality problems such as voltage sags, which arise due to a fault or a pulsed load, can cause interruptions of critical loads. This can be of a serious concern for the survivability of a combat ship. A series voltage injection type flywheel energy storage system is used to mitigate voltage sags. The basic circuit consists of an energy storage system, power electronic interface and a series connected transformer. In this case the energy storage system consists of a flywheel coupled to an induction machine. The power electronic interface consists of two voltage sourced converters (VSC) connected through a common DC link. The flywheel stores energy in the form of kinetic energy and the induction machine is used for energy conversion. Bi-directional power flow is maintained by regulating the DC bus voltage. Indirect field oriented control with space vector PWM is used to control the induction machine. Sinusoidal PWM is used for controlling the power system side VSC. This paper presents the modeling, simulation and analysis of a flywheel energy storage system and with a power converter interface using EMTDC..

**Keywords** – SPS, FESS, PSCAD/EMTDC, VSC, Field Oriented Control, Space Vector PWM, and Sinusoidal PWM.

## I. INTRODUCTION

The U.S Navy is looking for methods to maximize survivability of its combat ships during battle conditions and optimize operation during routine sailing [1]. A shipboard power system (SPS) is a stiff, isolated power system. Power is generated locally and distributed over short distances, so the entire system is impacted equally by voltage transients. Power quality problems such as voltage sags, which arise due to a fault or a pulsed load, can cause interruptions of critical loads [2]. This can be of a serious concern for the survivability of a combat ship. Series voltage compensation with energy storage is an effective way to mitigate voltage sags [3]. The basic idea is to store energy during normal condition and utilize it to mitigate sags. Energy storage can be a battery, SMES or a flywheel. The advantages such as cost, ruggedness, more number of charge-discharge cycles and high power density makes flywheel a viable alternative to SMES or a battery.

A flywheel stores energy in the form of kinetic energy. The amount of energy stored varies linearly with the mo-

ment of inertia of the flywheel, and the square of its angular velocity [3,4,5]. Flywheels can be designed for low speed or high-speed operation. With the advent of new composite materials and magnetic bearings technology, flywheels have overcome most of their physical limitations on the amount of energy stored. However the gains with these materials are offset by initial costs. A low speed flywheel has advantages of lower cost and the use of proven technologies, when compared to a high-speed flywheel system. The main disadvantages are less stored energy per volume, higher losses and increased volume and mass.

A low speed flywheel coupled to an induction machine is explored in this paper. The induction machine is used for bi-directional conversion of energy to the flywheel. A voltage sourced converter (VSC) is used to interface the induction machine with storage system. Indirect field oriented control with space vector PWM is used to control the induction machine.

A voltage sourced converter-based static series compensator is used for voltage sag correction. The power electronic interface facilitates the bi-directional flow of energy for charging and discharging the flywheel. Sinusoidal PWM is used for controlling the static series compensator.

This paper presents the modeling and simulation of a flywheel energy storage system (FESS) with a power converter interface in PSCAD/EMTDC [6] and analysis of its performance for typical voltage sags on a shipboard power system.

## II. BASIC CIRCUIT AND OPERATION

The basic circuit consists of an energy storage system, power electronic interface and a series transformer as shown in Fig.1.

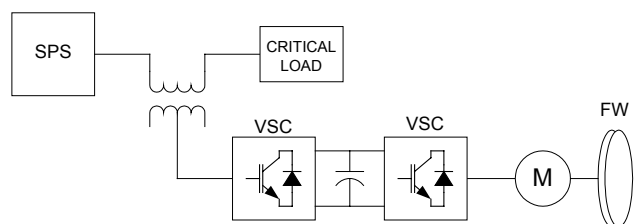


Fig. 1 Basic Circuit Diagram

The energy storage system in this case is a flywheel coupled to an induction machine. The power electronic interface consists of two VSC's connected through a common DC link. One VSC interfaces with the energy storage system and the other interfaces with the shipboard power system.

During charge mode the VSC interfacing the shipboard power system runs as a rectifier and the other as an inverter charging the flywheel to its rated speed. Once the flywheel reaches its rated speed the storage system is in a stand-by mode and ready to discharge when the critical load sees a voltage sag. During discharge mode the VSC interfacing the shipboard power system runs as an inverter, transferring the stored energy to the ac system for voltage sag correction. The other VSC runs as a rectifier thereby decreasing the flywheel speed.

The sag detection and power electronic interface control determines the dynamic response of the energy storage system.

### III. MODELING

The field oriented AC drive model consists of an induction machine model, an indirect field oriented controller, and a space vector PWM pulse generator. The basic layout is shown in Fig. 2.

#### A. Induction Machine Modeling

The induction machine is modeled in a synchronously rotating D-Q reference frame using the following state space flux equations [7].

$$p \cdot \lambda_{qs} = V_{qs} + (\lambda_{qs} \cdot L_r - \lambda_{qr} \cdot L_m) \cdot \frac{R_s}{L_s \cdot L_r \cdot \sigma} - \lambda_{ds} \cdot \omega_e \quad (1)$$

$$p \cdot \lambda_{ds} = V_{ds} + (\lambda_{ds} \cdot L_r - \lambda_{dr} \cdot L_m) \cdot \frac{R_s}{L_s \cdot L_r \cdot \sigma} + \lambda_{qs} \cdot \omega_e \quad (2)$$

$$p \cdot \lambda_{qr} = - \left[ (\lambda_{qr} \cdot L_s - \lambda_{qs} \cdot L_m) \cdot \frac{R_r}{L_s \cdot L_r \cdot \sigma} \right] - \lambda_{dr} \cdot (\omega_e - \omega_r) \quad (3)$$

$$p \cdot \lambda_{dr} = - \left[ (\lambda_{dr} \cdot L_s - \lambda_{ds} \cdot L_m) \cdot \frac{R_r}{L_s \cdot L_r \cdot \sigma} \right] + \lambda_{qr} \cdot (\omega_e - \omega_r) \quad (4)$$

This model computes the stator currents from the measured voltages at the inverter terminals. The stator currents are represented as three dependent current sources con-

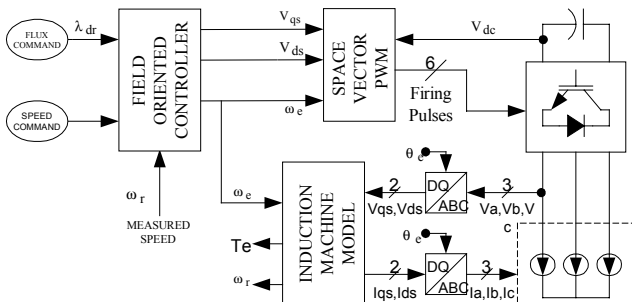


Fig. 2. Machine side layout

nected in wye, added into the electrical circuit as shown in the Fig. 2. Flywheel is modeled as an additional inertia connected to the rotor shaft of the induction machine model.

#### B. Field Oriented Controller (FOC)

The basic concept of field orientation is to align the rotor flux space vector along the D axis so that the Q axis component of it is zero at all times. With this alignment, torque and flux of the machine can be controlled instantaneously and independently as occurs in a separately excited DC machine. There are two common methods to implement this, depending on the way the rotor flux angle is obtained [8]. One is by directly computing it from the flux measurement using Hall effect sensors called Direct FOC. The other method computes the rotor flux angle based on the measured rotor position and slip relationship. This method is called Indirect FOC. An indirect field orientated controller that uses voltage as control variable is implemented in EMTDC for this investigation. The controller was initially developed in MATLAB and interfaced to the power converter model in EMTDC. Once the controller design was completed, it was then implemented directly in EMTDC. The controller uses flux and torque commands as inputs, and produces compensated flux responses for correctly handling flux variations. The torque command comes from a speed controller.

#### C. Space Vector Pulsewidth Modulator

Space vector PWM technique is used for controlling the machine side converter. It has advantages such minimum switching losses, decreased harmonic distortion and greater utilization of DC bus compared to sinusoidal PWM [9].

A space vector pulsewidth modulator has been modeled in EMTDC. Fig. 3 shows the basic layout of the modulator model. The modulator fabricates the space vector PWM pulses for a commanded DQ voltage, output frequency, switching frequency and DC bus voltage.

The active and zero times ( $T_a, T_b$  and  $T_0$ ) are computed by using a MATLAB script interfaced to EMTDC as shown in the figure. An asynchronous timer is required which acts as a time reference for sampling and pulse fabrication. The asynchronous timer resets when the commanded space vector moves to a new sector. The MATLAB interface outputs the switching times and the current sector in which the space vector is. A sector pulse

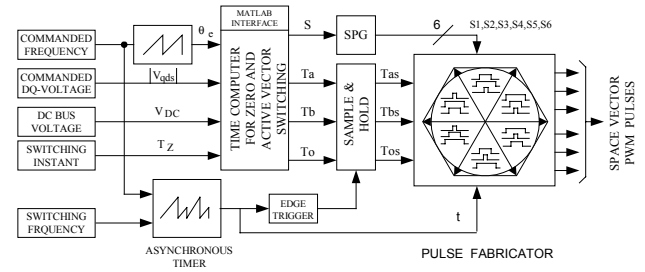


Fig. 3. Space vector PWM layout.

generator (SPG) generates pulses for sector reference. Using the time reference, the sampled switching instants, and the SPG, the pulse fabricator generates space vector PWM pulses.

A smooth transition from Space vector to six-step operation is also incorporated in the modulator.

#### D. Power system Modeling

The shipboard power system is modeled in EMTDC as a simple radial system with a source, a bus and a load as shown in Fig.2. Faults are initiated in the system so that the critical load experiences voltage sags. A sinusoidal pulse width modulator is modeled in EMTDC to control the VSC on the SPS side. For a given amplitude modulation index, phase angle reference, frequency and DC bus voltage it generates firing pulses for the converter. A LC filter bank is used to smooth the injected voltage.

## IV. CONTROL SYSTEM

The outer control system consists of a sag detector, sag corrector and energy control system as shown in Fig. 4. The outer control system determines the energy to flow in and out of the storage system according to the need. The outputs of this component are amplitude modulation index and phase angle inputs for the sinusoidal pulselwidth modulator and torque command for the FOC.

#### A. Sag detector

The sag detector detects the voltage sag and activates the control system for sag correction. The output of it is a pulse with duration equal to the duration of voltage sag. The inputs are the voltages measured on the SPS side. The

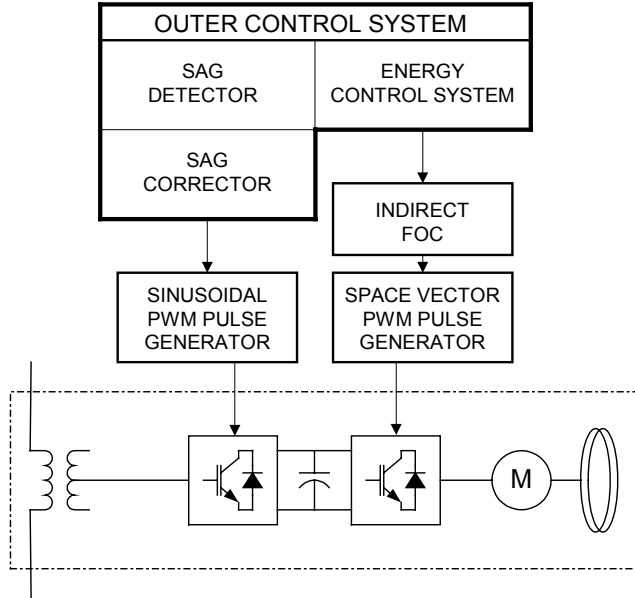


Fig. 4: Space vector PWM layout.

measured voltages are converted to DQ space vector in synchronously rotating reference frame. The magnitude of the space vector is compared to a reference value (1.0pu). The detector can give accurate result only for balanced voltage sags. The layout of the sag detector is shown in the Fig. 5.

#### B. Sag correction

Sag correction is done by commanding a negative torque to the FOC which forces the induction machine to convert the stored energy to electric power, resulting in an increase of DC bus voltage. The VSC on the SPS side is controlled to regulate the DC bus voltage to a reference value as shown in Fig. 5, so when the dc bus voltage increases, it will transfer energy from the DC bus to the power system. During normal conditions the VSC on the SPS side is forced to run as a rectifier keeping the energy storage system in stand-by mode. When the DC bus voltage increases due to energy conversion the VSC on the SPS side is forced to run as an inverter and correct the voltage sag.

#### C Energy Control System

Fig. 6 shows the basic layout of the energy control system. The output is a torque command to the indirect field oriented controller, which is the sum of outputs from three main control blocks: DC voltage control, speed control and sag correction control. The torque command  $T_C$ , is an input to the indirect field oriented controller in Fig.2.

A proportional integral feedback control is used for controlling rotor speed and DC bus voltage. Speed control, the slowest controller, is used for charging the flywheel to its charge speed when the sag is cleared. If the sag detector detects a sag, SD goes high. This results in bypassing the speed and DC bus voltage controllers, such that  $T_C$  equals  $T_{SAG}$ , and improves the response time.

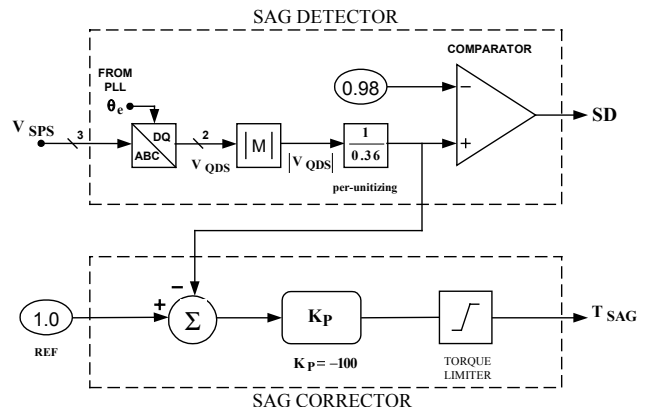


Fig. 5: Sag Detector and Sag Correction Control System Layout

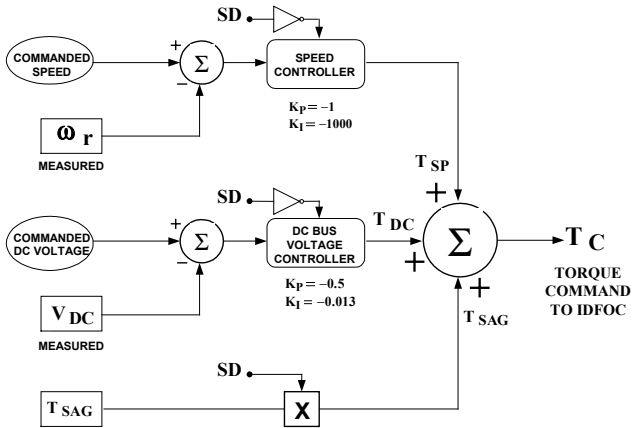


Fig. 6 Energy Control System Layout

## V. SIMULATION RESULTS

The FESS performance is analyzed by creating a three-phase fault at the location shown in Fig. 7. The system model and component ratings are based on a laboratory test system that will be described in a future paper. The FESS based series compensator will be connected into the model power system.

The fault results in a balanced voltage sag of 63% on the SPS side of the series transformer. The depth of the voltage sag depends on this distance of the fault from the bus. The fault occurs at 1.5sec into the simulation, with duration of 20 cycles.

Fig. 8 shows the detection of the voltage sag by the sag detector. The variable SD is zero until the fault is detected and then goes to logic one when the SPS voltage is out of tolerance. The output VdqSPS is the per unit magnitude of SPS side voltage space vector, and VabcSPS is the per unit RMS voltage.

Note that the space vector voltage magnitude changes much more quickly since it is based on instantaneous quantities, and not averaged over a cycle as the RMS voltages are. Therefore, a RMS voltage reference based sag detector will react more slowly, and hurt the response of the system. The space vector based DQ voltage is used to provide faster, more accurate detection of the voltage sag in the system described in this paper.

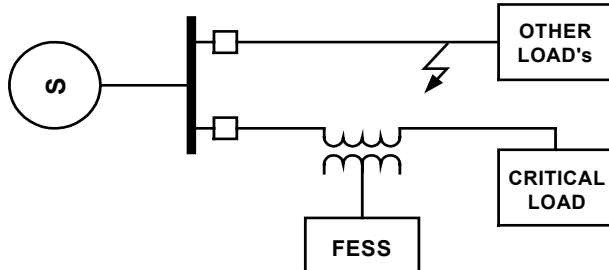


Fig. 7. Static Series Compensator Test System Layout

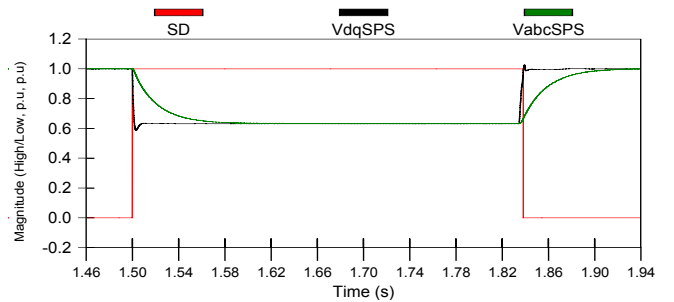


Fig. 8. Sag detector response.

When SD goes high in Fig. 8, the sag corrector is activated. The speed and DC bus controllers are bypassed. The sag corrector commands a negative torque,  $T_{SAG}$ , to the indirect field oriented controller, for energy conversion. The flywheel was in standby mode, running at 346 rad/s, until SD goes high. Fig. 9 shows the flywheel slowing down due to the negative torque command. Fig. 10 shows the DC bus voltage variation during energy reversal. Note that the dc bus voltage rises as energy is transferred from the flywheel to the dc bus.

Fig. 11 shows the power flow measured at the machine terminals and at the secondary of the series transformer. Note the peak power transfer in this case is approximately 6 kW.

Fig. 12 shows the per-unit RMS voltage on the critical load side and the SPS side. The RMS voltage on the SPS side was initially at 1.0p.u. A voltage sag of 63% is seen, lasting for 20 cycles.

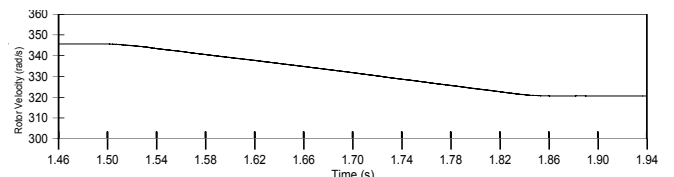


Fig. 9. Variation of rotor angular velocity.

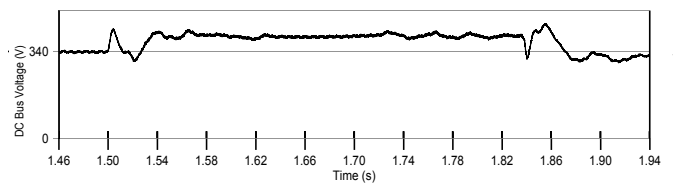


Fig. 10. Variation of DC bus voltage.

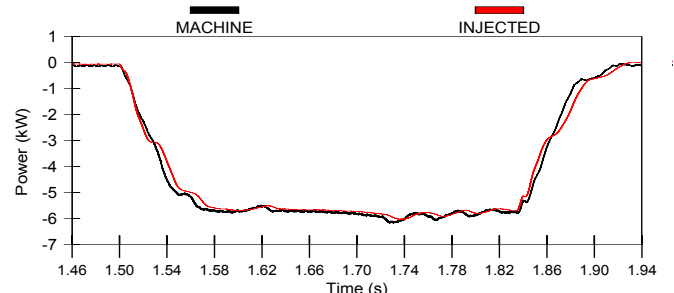


Fig. 11. Power measured flowing into the machine and into the SPS.

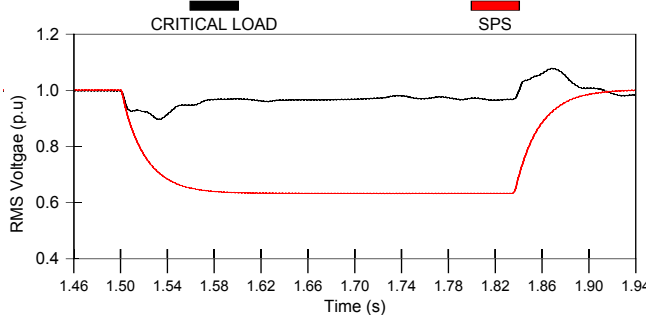


Fig. 12. RMS voltages measured at the critical load side and SPS side.

Figures 13 and 14 show the phase to ground voltages on the SPS side and critical load side respectively. The FESS responded within 2 cycles to keep the critical load voltage within the 5% tolerance (i.e. the sag is corrected to 0.95 per unit, not 1.0 per unit). The sag correction can be done for 0% tolerance but it will result in overvoltages at the end of the sag, with the potential to cause insulation damage. In this case, the critical load voltage was regulated below 5% of the nominal.

Fig. 15 shows the phase to ground voltage on the critical load side, SPS side, phase A current and the injected voltage by the VSC on the SPS side.

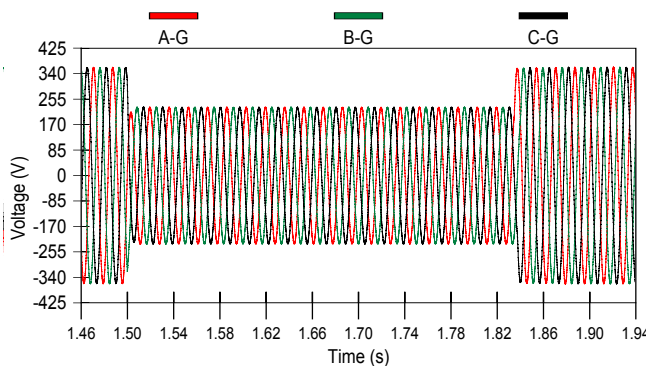


Fig. 13. Phase-Ground voltages measured on the SPS side.

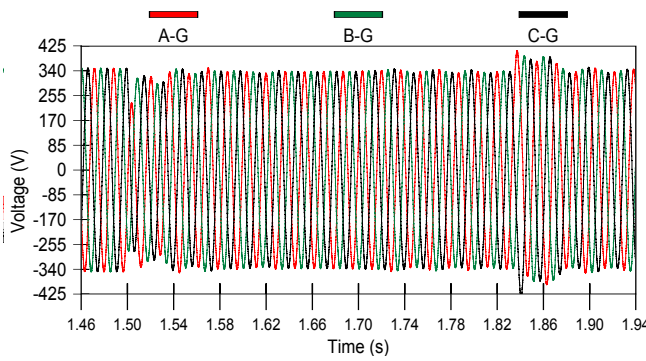


Fig. 14. Phase-Ground voltages measured at the critical load.

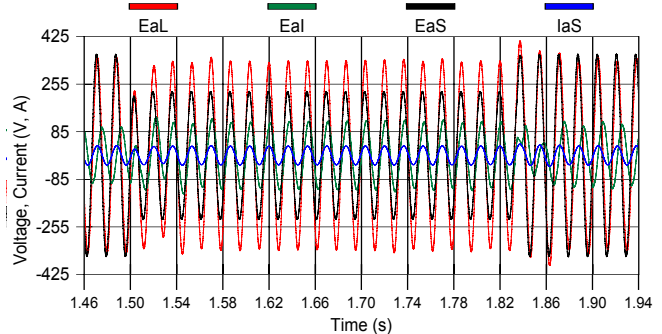


Fig. 15. Phase A-Ground voltage at the critical load and SPS, voltage across the series transformer and Phase A line current.

## VI. CONCLUSION

The modeling and analysis of flywheel energy storage system (FESS) based static series compensator for a shipboard power system has been presented. A control system based on negative torque command, which is a scaled error of the difference between SPS side of the DQ voltage and its reference for sag correction has been presented. An energy control system that regulates the DC bus voltage and charges the flywheel has been described.

The power system and the power converters are modeled using EMTDC, along with the induction machine and flywheel model. An indirect field oriented control for the flywheel induction machine was also modeled in EMTDC. The space vector PWM scheme to generate firing pulses for the flywheel converter was modeled in MATLAB and interfaced to the switching device models in EMTDC. The overall energy management scheme, the sag detector, and the sag corrector were all modeled in EMTDC, along with the control scheme for the shipboard power system side VSC.

The response of the compensator to a voltage sag was presented. The advantages of a DQ based sag detector over RMS voltage has been shown. The instantaneous voltages are compensated within 2 cycles to keep the voltage tolerance within 5% of rated voltage.

The main advantage of this FESS is low cost and high energy density. It can mitigate long duration voltage sags efficiently. Future work will include a comparison with a laboratory flywheel interfaced to an analog model power system.

## ACKNOWLEDGEMENT

This work presented here was funded by the Office of Naval Research, USA, under Grant N000140010477.

## APPENDIX

TABLE I  
SYSTEM DATA

Shipboard Power system	3Ph, 480V, 60Hz, 50kVA
Series Transformer	480/480V, 50kVA, 10%
LC Filters	10mH, 20μF
Critical Load	Passive, 3Ph-Resistive load, 10Ω
Other Loads	Passive, 3Ph-RL load, 5Ω, 10mH
Line Impedance to other loads	0.2Ω, 1mH
DC Bus	340V, 2 x 1000μF center tapped
Flywheel Inertia	9.911 kg·m <sup>2</sup>
Induction Machine	240V, 60Hz, 23.8A, 10hp, 4pole and 1755RPM
SVPWM switching frequency	1kHz
SPWM switching frequency	10.8kHz

## REFERENCES

- [1] A. T. Adediran, H. Xiao and K.L. Butler, "Fault studies of an U.S. Naval Shipboard Power System", *NAPS, University of Waterloo, Canada*, October 2000.
- [2] M. H. J. Bollen, Understanding Power Quality Problems, IEEE Press, 2000
- [3] R. S. Weissbach, G. G. Karady and R. G. Farmer, "Dynamic Voltage Compensation on Distribution Feeders using Flywheel Energy Storage" *IEEE transactions on Delivery*, Vol.14, No.2, April 1999.
- [4] H. Akagi, "Large Static Converters for Industry and Utility Applications," *Proceedings of the IEEE*. Vol. 89, No. 6, June 2001.
- [5] H. Akagi and H. Sato, "Control and Performance of a Doubly-Fed Induction Machine Intended for a Flywheel Energy Storage System," *IEEE Transactions on Power Electronics*. Vol. 17, No. 1, January 2002.
- [6] "PSCAD/EMTDC User Manual.", HVDC Manitoba, Canada.
- [7] B. K. Bose " Modern Power Electronics and AC Drives" 2<sup>nd</sup> edition, Prentice Hall PTR, 2002, pp. 322-349, 169-174 and 700-710.
- [8] D. W. Novotny and T. A. Lipo " Vector Analysis and Control of AC Drives." 2<sup>nd</sup> edition, Oxford Science Publications, 1997.
- [9] H. W. Van Der Broeck, H. C. Skudelny and G. V. Stanke, "Analysis and Realization of a Pulsewidth Modulator Based on Voltage Space Vectors" *IEEE transactions on Industry Applications*, Vol.24, No.1, January/February 1988.

## BIOGRAPHIES

**Satish Samineni** received the B.E degree in electrical and electronics engineering from Andhra University college of Engineering, Visakhapatnam, India. He is presently pursuing his Master's degree in Electrical Engineering at the University of Idaho, Moscow, ID. His research inter-

ests include power electronics, power system protection and drives.

**Brian K. Johnson** received the Ph.D. degree in electrical engineering from the University of Wisconsin-Madison in 1992. He is currently an associate professor in the Department of Electrical and Computer Engineering at the University of Idaho, Moscow, ID. His interests include HVDC transmission, FACTS, Custom Power technologies, energy storage, power systems applications of superconductivity, power system protection and electromagnetic transients in power systems. Dr. Johnson is a member of CIGRE and is a professional engineer in Wisconsin and Idaho.

**Herbert L. Hess** received the Ph.D. degree in electrical engineering from the University of Wisconsin-Madison in 1993. He is currently an associate professor in the Department of Electrical and Computer Engineering at the University of Idaho, Moscow, ID. His research interests include power electronics, electric machines and drives and power quality.

**Joseph D. Law** received the Ph.D. degree in electrical engineering from the University of Wisconsin-Madison in 1991. He is currently an associate professor in the department of Electrical and Computer Engineering at the University of Idaho, Moscow, ID. His research interests include electric machines, power electronics and electrical disturbances in power systems.